Sensors & Transducers, Vol. 178, Issue 9, September 2014, pp. 14-19

Sensors & Transducers

A New North-seeking Method Based on MEMS Gyroscope

Yu Liu, Song Liu, Changwen Wang, Le Wang
Institute of Optical Communication Technology, Chongqing University of Posts and Telecommunications, Chongqing 400065, China
Tel.: 13883158002, fax: 021-62460380
E-mail: looseliu@126.com

Received: 10 June 2014 /Accepted: 29 August 2014 /Published: 30 September 2014

Abstract: In this paper, a new north-seeking method based on a low-cost Micro-Electro-Mechanical System (MEMS) gyroscope sensor has been proposed, which can solve the problem of long measurement time and low precision in north-seeking application. With this method the system has achieved an accuracy of approximately 2^o with respect to the North orientation. In order to achieve this accuracy, firstly we characterized the bias errors by using Allan variance; secondly an EKF filter was designed to compensate these errors properly, and finally the offset angle with respect to the North orientation was estimated properly by the experimental data. The results of experiment show that this new method is better than the universal north-seeking scheme in measurement time and the stability of the accuracy. *Copyright © 2014 IFSA Publishing, S. L.*

Keywords: MEMS gyroscope, North-seeking, Allan variance, EKF, Bias compensation.

1. Introduction

Geographic location information is a key factor in people's daily life, thus the research about machine indicating the Geographic orientation is of great significance. North seeking is to find the angle related to the Earth's north. Currently there are two mainly measurements to find the North on the market, electronic magnetometer and the inertial gyroscope compass. Electronic magnetometer can reach several mrads heading accuracy, but its accuracy can be disturbed easily by the surrounding material of iron or electromagnetic environment, which reduces its application range, such as it is not suitable for the indoor environment or complex electromagnetic environment. INS gyrocompass can solve these problems efficiently, and also can maintain high accuracy. However, gyrocompass systems often use tactical level gyroscope to conduct the north seeking measurements, such as fiber optic gyroscope, liquid floating gyroscope and laser gyroscope [1-2]. These gyroscopes are usually high cost and great volume, which prevent it from applying to the most of the positioning system on the market.

Compared with the common sensors or some positioning units, Micro-Electro-Mechanical System (MEMS) gyroscope has a smaller size, lighter weight and lower cost. With the rapid development of MEMS technology, precision and stability of MEMS sensors have been improved substantially in the last three years. MEMS inertial sensor technology provide a solution in cost, size and strength [3], but limited by the mechanical precision, the accuracy of MEMS gyroscopes is often affected by time, temperature and random drift. In [4-6], the measurement error of the gyroscope sensor can be compensated for by carouseling.

Aiming at the characteristics of MEMS gyroscope that output data can be easily affected by random drift and temperature, a new North-seeking method using MEMS gyroscope is proposed. Allan variance method is used to distinguish each random error of the MEMS gyroscope; and in order to compensate these errors, an EKF filter is used to process the gyroscope data; what's more, for compensating the effect of gravity on the measurement, a sequence of rotations was conducted in our approach.

The paper is organized as follows. Firstly, the theoretical background of this paper is presented in Section 2. The new north-seeking approach and measurement setup is showed in Section 3 while Section 4 analyses the results of experiment. Finally, Section 5 is the conclusion.

2. Theoretical Background

2.1. Allan Variance

Allan variance method is proposed by the U. S. National Bureau of Standards, David Allan in the 1960s [7]. Allan variance is a time-domain analysis; its theoretical foundation is that the output of linear systems is distributed normally by one or more white noise. Assuming the sampling interval is T_s, while the total sampling period is T, then the total number of data points can be obtained as a data sample. The total number is $N = T / T_s$.

All data samples are divided into K subsets equably according to the time sequence, the number of each subset is n, and the average time for each subset $\tau(n) = nT_s$. Then the covariance of each subset can be presented as

$$\overline{\Omega}_k(\tau) = \frac{1}{n}\sum_{i=1}^{n}\Omega_i^k, \quad (1)$$

where $\overline{\Omega}_k(\tau)$ represents the mean of the kth subset, while Ω_i^k indicates the ith point of kth subset. The Allan covariance can be computed as

$$AVAR^2(\tau) = \frac{1}{2}E[(\overline{\Omega}_{k+1}(\tau) - \overline{\Omega}_k(\tau))^2], \quad (2)$$

where $AVAR^2(\tau)$ denotes the Allan covariance when the coverage time is τ, and E is a sign of calculating covariance. Regard the mean time τ as independent variable, we can get Allan variance curve with the change of τ. Several common errors are related to different average time, which means they also correspond to different slope. Table 1 lists the correspondence between the three kinds of common error coefficients and Allan covariance; these correspondences can determine three kinds of noise factors.

Before collecting gyroscope data, the gyroscope should be preheated to ensure it work well. The sampling frequency is 100 Hz, while the total sampling time is 7 h. MATLAB software is used to process gyroscope data, the raw data collected in static state is showed in Fig. 1, and Fig. 2 is the calculated Allan variance curve.

Table 1. The relationship between Allan standard deviation and common error coefficient.

Allan standard deviation	Error coefficient	Curve slope
$AVAR(\tau) = \sqrt{3}Q / \tau$	Quantization error Q	-1
$AVAR(\tau) = R / \sqrt{\tau}$	Rate random walk R	-1/2
$AVAR(\tau) = 0.664B$	Zero offset instability B	0

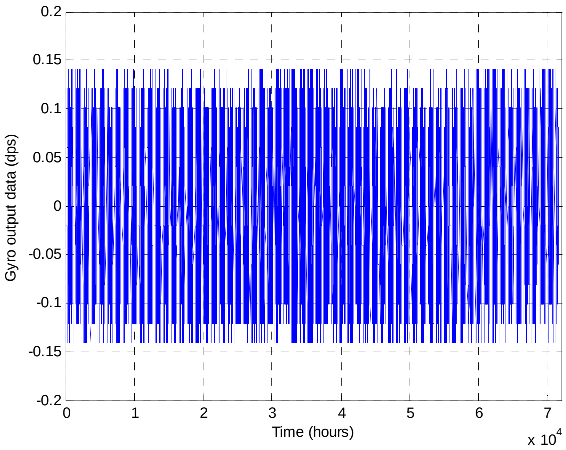

Fig. 1. Gyroscope static data in 7 hours.

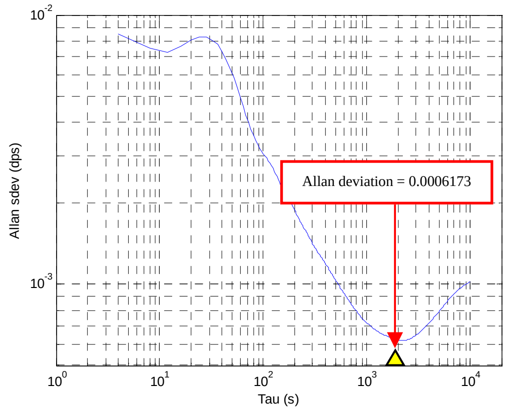

Fig. 2. Allan variance curve of Gyroscope sensor.

To obtain corresponding slope value, the Allan variance should be processed by polynomial fitting, and then we can get all noise factors. From the Allan variance showed in Fig. 2 it can be seen that the zero bias instability is nearly 0.00061 °/s. The World Geographic System 1984 (WGS84) released that the Earth's rotation rate $\omega_e = 72921 \times 10^{-11} rad/s \approx 4.178 \times 10^{-3} \deg/s$ [8]. Therefore, the noise level of the gyroscope sensor is low enough to measure the rotation rate of the Earth, and it also means that it can be used to find the true North.

2.2. Extended Kalman Filtering

The mathematical foundations of Kalman filter were presented between 1959 and 1961 [9]. Kalman filter offered an optimal estimation for linear system models with additive independent white noise. But in fact most systems are nonlinear, such as the north-seeking measurement system. The EKF represented as an available solution, which can apply to nonlinear systems. EKF is a kind of recursive estimation, i.e. as long as we know the estimate value of previous state and the observed value of current time, and then the estimate value of current state can be calculated.

The operation of EKF consists of two stages: prediction and update [10]. In prediction stage, the filter makes an estimation of the current state by using the previous state; and in update phase, the observation value of current state is used to optimize predictive value of observations obtained in the prediction stage. From the viewpoint of the system we can treat the gyroscope drift as a constant value, periodic component and Gaussian white noise. Firstly, the state and output equations of the EKF filter can be denoted as

$$X_k = AX_{k-1} + BV_k \, , \tag{3}$$

$$Y_k = CX_k + W_k \, , \tag{4}$$

where A represents state transition matrix, B is the error correlation matrix, and C indicates measurement noise matrix, while statistical properties of W_k and V_k are $W_k \sim N(0, Q_k)$, $V_k \sim N(0, R_k)$. We assume that the system state vector

$$X_k = [\hat{x}_k, \hat{x}_{k-1}]^T \, , \tag{5}$$

the processing error $V_k = [\alpha_k, 0]^T$, W_k is estimating error of the model. Then we can get $x_k = \hat{x}_k + W_k$. According to the above system equations, the EKF filter recursive expression can be written as

$$\begin{cases} \hat{X}_{k|k-1} = A\hat{X}_{k-1|k-1} \\ \hat{X}_{k|k} = \hat{X}_{k|k-1} + K_k[Y_k - C_k\hat{X}_{k|k-1}] \\ K_k = P_{k|k-1}C^T[CP_{k|k-1}C^T + R]^{-1} \\ P_{k|k-1} = AP_{k|k-1}A^T + BQ_{k-1}B^T \\ P_{k|k} = [I - K_kC]P_{k|k-1} \\ \hat{Y}_k = C\hat{X}_{k|k} \end{cases} , \tag{6}$$

where $\hat{X}_{k|k-1}$ denotes one step estimation of filter state, and $\hat{X}_{k|k}$ represents state of filter at time k, while K_k is the gain matrix of filter at time k, R indicates measurement error variance of system, Q is the process error variance, $P_{k|k}$ denotes covariance matrix of filter error, $P_{k|k-1}$ is covariance matrix of one step estimation error, the initial value of P is $\begin{bmatrix} 1 & 0 \\ 0 & 1 \end{bmatrix}$, $\hat{Y}_k$ represents the output of filter at time k.

3. A New North-seeking Method

3.1. Two Positions North-seeking Principle

The mainly principle of Gyroscope North-seeking is that the Earth's rotation rate can be measured by gyroscope, and then we can find the angle between the gyroscope sensitive axis and true north [11]. North-seeking principle based on gyroscope is depicted in Fig. 3, a geographic coordinate is established at gyroscope location P, X_e-axis positive toward geographic east direction, Y_e-axis positive toward geographic north direction, while Z_e-axis is the direction that toward the sky and perpendicular to the horizontal plane.

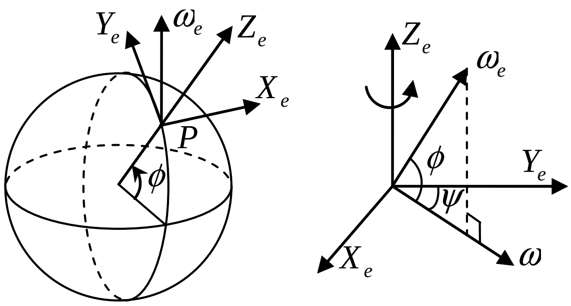

Fig. 3. North-seeking principle based on Gyroscope.

Assuming the angle between the initial direction of the gyroscope sensitive axis and true North is ψ, the latitude of the point P is ϕ, and Earth's rotation rate is ω_e, ω towards the direction of gyroscope sensitive axis. The output value of gyroscope at position 1 is ω_1; then we rotate gyroscope sensitive axis 180° to position 2 by using the rotation table, and the output value of gyroscope is ω_2 at this time.

$$\omega_1 = \omega_e \cos\phi \cos\psi + \varepsilon(t_1) \, , \tag{7}$$

$$\omega_2 = -\omega_e \cos\phi \cos\psi + \varepsilon(t_2) \, , \tag{8}$$

where $\varepsilon(t_1)$ and $\varepsilon(t_2)$ represent the bias value of gyroscope at time t_1 and t_2 respectively. In the short-term measurement, the effects of noise and temperature variation on the gyroscope data are considered approximately identical. Form (7), (8) the angle ψ between the gyroscope sensitive axis and the true north can be calculated as

$$\psi = \arccos\left(\frac{\omega_1 - \omega_2}{2\omega_e \cos\phi}\right) \tag{9}$$

3.2. Improved North-seeking Method

36 experiments were conducted by using the universal two-position north seeking scheme. In each set of experiment, the sensitive axis of sensor was rotated 10° in clockwise direction by horizontal turntable. All the tests carried out in this article were run in Chongqing, its latitude is $\varphi \approx 29.5^\circ N$, and the sampling frequency of the gyroscope sensor is about 50 Hz. According to equation (7), ignoring the effects of temperature and zero drift, we got 36 values of $\omega_e \cos\phi \cos\psi$. The theoretical analysis on these experimental data is showed in Fig. 4.

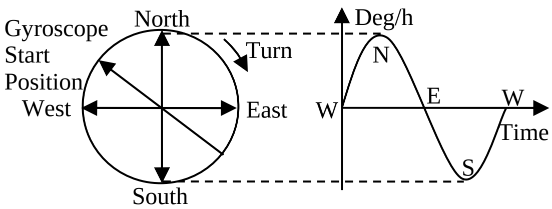

Fig. 4. Theoretical analysis on experimental data.

According to the theoretical analysis of Fig. 4, when the MEMS gyroscope was in the north direction, the maximum value of $\omega_e \cos\phi \cos\psi$ can be achieved; when the MEMS gyroscope was in the south direction, the minimum value of $\omega_e \cos\phi \cos\psi$ can be obtained; when the MEMS gyroscope was in the east or west direction, the value of $\omega_e \cos\phi \cos\psi$ will be zero; the curve achieved can be depicted as

$$y = A\sin(\omega t + \varphi), \tag{10}$$

where $A = \omega_e \cos\phi$, the frequency of curve $\omega = \pi/18$, at this time the angle between gyroscope sensitive axis and the north direction can be obtained by calculating the phase of the sine curve φ.

3.3. Measurement Setup

As the gyroscope, we used a demo of VTI's SCC1300-D02 MEMS angular rate sensor. The package of the sensor is depicted in Fig. 5, while some specifications of SCC1300-D02 are shown in Table 2.

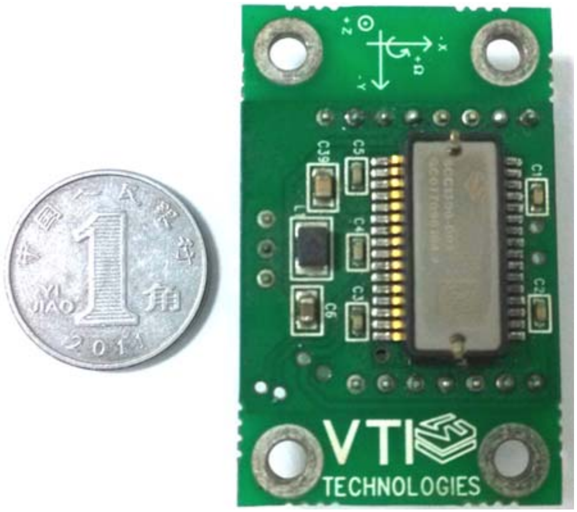

Fig. 5. The MEMS Gyroscope package.

Table 2. Gyroscope sensor specifications.

Parameter	Value	Unit
Operating range	±100	°/s
Angular random walk (ARW)	0.45	$°/\sqrt{h}$
Offset instability	< 1	°/h
Noise (RMS)	0.06	°/s
Sensitivity	50	LSB/(°/s)
Quantization	0.05	°/h

Table 3 summarizes some specifications of the gyroscope. It can be seen that the performance of the sensor meets the requirements for north finding, and if the errors that affect the output data are properly compensated for, it can achieve a high accuracy in detecting the Earth's rotation rate [12].

The measurement structure is shown in Fig. 6. In order to avoid the effects of gravity on the gyroscope data, the MEMS gyroscope is placed on the horizontal rotating stage, so that the gyroscope sensitive axis parallels to the Earth's surface. Data and power cables of the gyroscope and host computer are connected for communication through the slip ring of horizontal rotary table. Finally the host computer controls rotating table, and collects the output data of gyroscope.

Table 3. Experimental results at different initial positions of gyroscope sensitive axis.

Number	Theoretical value (deg)	Computed value (deg)
1	0	5.39
2	30	23.88
3	60	57.40
4	90	91.57
5	120	116.20
6	150	156.11
7	180	190.38

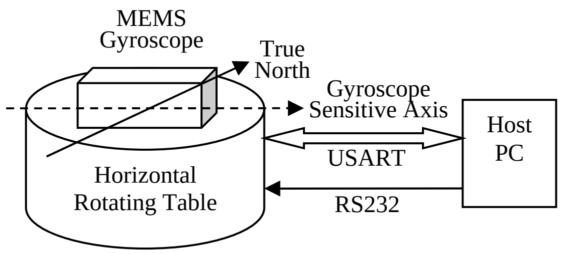

Fig. 6. Sketch map of the measurement structure.

4. Experimental Results

The experimental results are presented in Fig. 5. During the experiment the initial direction of MEMS gyroscope was toward the true north, and from the Fig. 5 it can be seen that the graphic drew by 36 sets of data also is accord with the consequence of theoretical analysis.

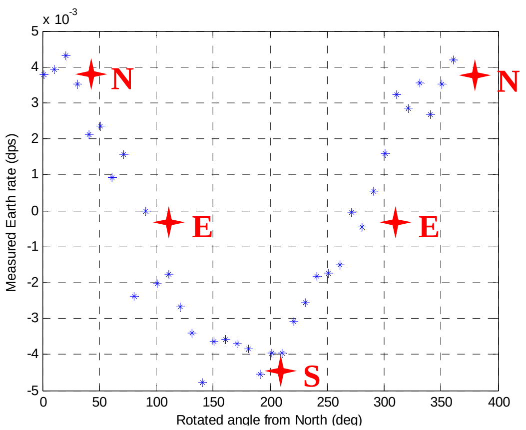

Fig. 7. The experimental result for 360° rotation spaced by 10°.

Then, for our next measurements we used an extended Kalman filter as depicted in Section 2. We used the same data as in Fig. 5 for verifying the validity of filter. Fig. 6 shows the comparison of the experimental data before and after filtering.

We can see from Fig. 6 that the results were very close between the output of the filter and the theoretical values of the Earth's rotation rate. The phase of the filtered curve can be computed by utilizing the theory denoted in Section 3. Some other experiments at different initial positions of gyroscope sensitive axis were conducted for investigating the stability and measurement accuracy of the north-seeking method. The experimental results are presented in Table 2.

As it can be seen from Table 2, the accuracy at East and West directions is better than North and south obviously. This is because of the fact that the slope of the curve is steeper, making the measurement more accurate. After approximately 2 hours the system can achieve the accuracy of nearly 2° with respect to the north orientation.

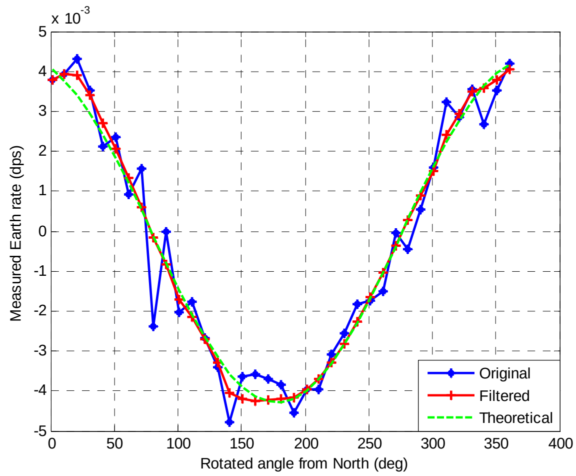

Fig. 8. The comparison of the experimental data before and after filtering.

5. Conclusions

This paper presented a new north-seeking method based on a low-cost MEMS gyroscope sensor. Error compensation methods taken for MEMS gyroscope consist in making the sensor parallel to the horizon to reduce the effects of gravity on the measurement, doing a sequence of rotation to compensate the zero bias errors, using an EKF filter to reduce the angular rate random walk. With the proposed method we achieved an accuracy of approximately 2° between the sensitive axis and the north direction.

Future work will be focused on improving the stability of the accuracy, shortening measurement time by using more efficient algorithm. In order to meet the actual application conditions, the north-seeking system combinating multiple gyroscopes maybe improve further the accuracy and stability.

Acknowledgements

This research is supported by National Natural Science Foundation (No. 51175335) and Natural

Science Foundation of Chongqing (No. CSTC-2012jj B40003), and is also thankful to Murata Technologies for providing the demo of the new SCC1300-D02 MEMS gyroscope.

References

[1]. Li D. H., Zhou F., Wu X. B., Research on two-position north-seeking method based on the Single axis FOG, *Advanced Materials Research*, 301, 2011, pp. 1489-1494.

[2]. Jiang Q. X., Ma X. H., Chen X. B., *et al*., North determining scheme by two-position for a FOG north seeker, *Journal of Chinese Inertial Technology*, 14, 3, 2006, pp. 1-5.

[3]. Weinberg M. S., Kourepenis A., Error sources in in-plane silicon tuning-fork MEMS gyroscopes, *Micro-Electro-mechanical Systems*, 15, 3, 2006, pp. 479-491.

[4]. Johnson B. R., Cabuz E., French H. B., *et al.*, Development of a MEMS gyroscope for northfinding applications, in *Proceedings of the IEEE/ION. IEEE Conference on Position Location and Navigation Symposium (PLANS)*, 2010, pp. 168-170.

[5]. Renkoski B. M., The effect of carouseling on MEMS IMU performance for gyroscopecompassing applications, *Massachusetts Institute of Technology*, 2008.

[6]. Bai Y. C., Li X. Q., Ma X. H., *et al*., High-precision north determining scheme based on rotation-modeulation technology, *Journal of Chinese Inertial Technology*, 18, 4, 2010, pp. 421-424.

[7]. D. W. Allan, The Allan variance, http://www.allanstime.com/AllanVariance/index.html.

[8]. Mularie W. M., Department of defense world geodetic system 1984, its definition and relationships with local geodetic systems, *National Geospatial-Intelligence Agency*, Tech. Rep., 2000, pp. 152.

[9]. Kalman R. E., Bucy R. S., New results in linear filtering and prediction theory, *Journal of Basic Engineering*, 83, 1, 1961, pp. 95-108.

[10]. Kalman filtering and neural networks, Ed. by Simon Haykin, *Wiley*, New York, 2001.

[11]. Bu J. J., Wei G. L., Li Y. J., *et al*., Two-Position Detecting Scheme for Gyroscope-Based North Seeker, *Journal of Chinese Inertial Technology*, 3, 2002, pp. 009.

[12]. Iozan L. I., Collin J., Pekkalin O., *et al*., Measuring the Earth’s rotation rate using a low-cost MEMS gyroscope, in *Proceedings of the Symposium Gyroscope Technology*, Karlsruhe, Germany, 2010.